5.3.2 Low carrier densities

At low carrier densities, the electron and hole distributions will be described by classical statistics. The distributions shown in Fig. 5.5(b) are drawn for this limit. In this situation the occupancy of the levels is small and we can ignore the $+1$ factor in eqn 5.8. The occupancies are then just given by Boltzmann statistics:

$$f(E) \propto \exp\left(-\frac{E}{k_B T}\right) . \tag{5.11}$$

Equation 5.11 will be valid for the electrons if E_F^c is large and negative. Exercise 5.9 explores this limit. It is reasonably obvious that it will be valid at low carrier densities and high temperatures.

The frequency dependence of the emission spectrum in the classical limit can be calculated if we assume that the matrix element in eqn 5.3 is independent of frequency. We can then evaluate all the factors in eqn 5.3 and obtain

$$I(h\nu) \propto (h\nu - E_g)^{1/2} \exp\left(-\frac{h\nu - E_g}{k_B T}\right) . \tag{5.12}$$

The $(h\nu - E_g)^{1/2}$ factor arises from the joint density of states for the interband transition (cf. eqn 3.24). The final factor arises from the Boltzmann statistics of the electrons and holes: see Exercise 5.8. The luminescence spectrum described by eqn 5.12 rises sharply at E_g and then falls off exponentially with a decay constant of $k_B T$ due to the Boltzmann factor. We thus expect a sharply peaked spectrum of width $\sim k_B T$ starting at E_g.

Figure 5.6 shows the photoluminescence spectrum of GaAs at a temperature of 100 K. The spectrum was obtained using 1.96 eV photons from a helium-neon laser as the excitation source. The spectrum shows a sharp rise at E_g due to the $(h\nu - E_g)^{1/2}$ factor in eqn 5.12, and then falls off exponentially due to the

At very low temperatures, the emission spectrum from a direct gap semiconductor begins to depart from the form predicted by eqn 5.12, even for very low carrier densities. This is caused by the formation of excitons, and the possibility of radiative recombination involving impurities.

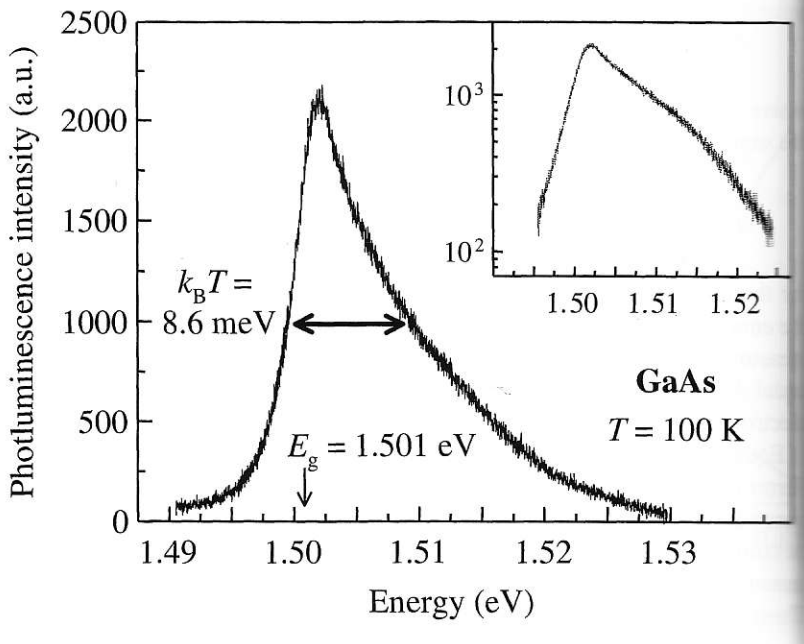

Fig. 5.6 Photoluminescence spectrum of GaAs at 100 K. The excitation source was a helium neon laser operating at 632.8 nm. The inset gives a semilogarithmic plot of the same data. (After A.D. Ashmore and M. Hopkinson, Personal communication)

Boltzmann factor. The full width at half maximum of the emission line is very close to $k_B T$, as expected. The fact that the high energy decay is exponential is clearly shown by the semilogarithmic plot of the same data given in the inset. The slope of the decay is consistent with the carrier temperature of 100 K.

5.3.3 Degeneracy

At high carrier densities, the classical limit will no longer be valid. The Fermi energies will be positive, and it is essential to use Fermi–Dirac statistics to describe the electron and hole distributions. This situation is called **degeneracy**.

In the extreme limit of $T = 0$, all the states up to the Fermi energy are filled and all states above it are empty. The Fermi energies can be calculated explicitly (see Exercise 5.10) and are given by:

$$E_F^{c,v} = \frac{\hbar^2}{2m^*_{e,h}} (3\pi^2 N_{e,h})^{\frac{2}{3}} . \tag{5.13}$$

The distribution of the carriers in this limit is shown in Fig. 5.7. Electron–hole recombination can occur between any states in which there is an electron in the upper level and a hole in the lower level. Recombination is thus possible for a range of photon energies between E_g and $(E_g + E_F^c + E_F^v)$. We therefore expect to observe a broad emission spectrum starting at E_g up to a sharp cut-off at $(E_g + E_F^c + E_F^v)$.

As finite temperatures the carriers will still be degenerate provided that $E_F^{c,v} \gg k_B T$, where $E_F^{c,v}$ is calculated using eqn 5.13. As T increases, the Fermi–Dirac functions smear out around the Fermi energies, and we expect to observe that the cut-off at $(E_g + E_F^c + E_F^v)$ will be broadened over an energy range $\sim k_B T$.

Figure 5.8 shows the emission spectrum of the III–V alloy semiconductor $Ga_{0.47}In_{0.53}As$ in the degenerate limit. $Ga_{0.47}In_{0.53}As$ has a direct gap of 0.81 eV at the lattice temperature T_L of 10 K. The spectra were obtained using the techniques of time-resolved photoluminescence spectroscopy described in Section 5.3.4 below. The figure shows the emission spectrum recorded at two different times after the sample has been excited with an ultrashort (< 8 ps) pulse from a dye laser operating at 610 nm. Each pulse has an energy of 6 nJ and is able to excite an initial carrier density of $2 \times 10^{24}\,\mathrm{m}^{-3}$.

The spectrum taken 24 ps after the pulse arrives rises sharply at E_g, and then shows a flat plateau up to $\sim 0.90\,\mathrm{eV}$. The spectrum then gradually falls off to zero at higher energies. The flat plateau is a signature of the degenerate carriers, while the high energy tail is an indication that the effective carrier temperature is higher than T_L due to the 'hot carrier' effect. In this case, the effective carrier temperature is 180 K. At 250 ps the carrier density is lower because a significant number of the electrons and holes have recombined, and the carriers have also cooled to a temperature of 55 K. At still longer times, the spectrum continues to narrow as the carrier density decreases and the carriers cool further towards the lattice temperature of 10 K. Eventually, the carrier density falls to the point where classical statistics are appropriate, and the emission only occurs at energies close to E_g. The analysis of this data is explored in more detail in Exercise 5.14.

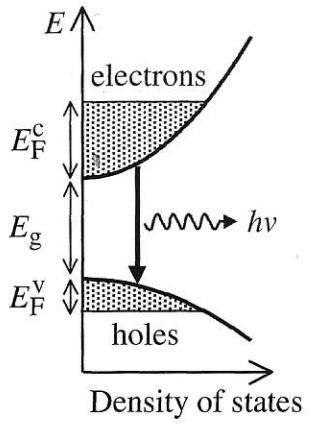

Fig. 5.7 Occupancy of the conduction and valence band states in the degenerate limit at $T = 0$. The electrons and holes have separate Fermi energies E_F^c and E_F^v respectively which are determined by the number of carriers injected into the bands. The conduction and valence bands are filled up to their respective Fermi levels, as shown by the shading.

Effective temperatures higher than T_L are possible because the carriers are not in full thermal equilibrium with the lattice. The carriers are 'hot' in the same sense that boiling water that has just been poured into a cold cup is hot: the temperatures are different initially, but gradually converge as heat flows from the water to the cup. In the case we are considering here, the electrons and holes are created high up the bands. This gives them a large amount of kinetic energy, which implies that their initial effective temperature is very high. This follows because the temperature is just a measure of the distribution of the carriers among the energy levels of the system. The temperature decreases rapidly as energy flows from the carriers to the lattice by phonon emission. The cooling towards T_L is therefore determined by the electron–phonon interactions in the material. Experimental values of the effective carrier temperature can be obtained by detailed modelling of the luminescence spectra.